Development of a theoretical model for predicting the thermal performance characteristics of a vertical pin-fin array heat sink under combined forced and natural convection with impinging flow

C.J. Kobus *, T. Oshio

School of Engineering and Computer Science, Oakland University, Rochester, MI 48309, USA

Abstract

A comprehensive theoretical and experimental study was carried out on the thermal performance of a pin-fin heat sink. A theoretical model was formulated that has the capability of predicting the influence of various geometrical, thermal, and flow parameters on the effective thermal resistance of the heat sink. An experimental technique was developed for measuring the thermal performance of the heat sink, and the overall convective heat transfer coefficient for the fin bundle. Experiments were carried out, and correlations obtained, for a wide range of parameters for pure natural convection and for combined forced and natural convection. The predictive capability of the theoretical model was verified by comparison with experimental data including the influence of various fin parameters and the existence of an optimum fin spacing.
© 2004 Elsevier Ltd. All rights reserved.

Keywords: Mixed; Combined; Convection; Heat sink; Heat transfer

1. Introduction

As power densities continue to increase, electronic component cooling becomes a more serious design problem. One of the most common means for cooling electronic modules is a finned heat sink that enhances convection heat transfer to ambient air. There are a variety of heat sink types, with differing fin geometries, and operating with natural or forced convection. A common

geometry is a pin-fin array heat sink. The research described in this paper focuses on the thermal performance of a pin-fin array heat sink which is oriented such that the air flow enters the fin-bundle perpendicular to the fin base (impinging flow). Also, the magnitude of the air velocity is small, such that both natural and forced convection are important.

The archival literature contains some experimental and theoretical studies on the thermal performance of pin-fin array heat sinks. Ledezma et al. [1] carried out an experimental, numerical, and theoretical study of the heat transfer from a pin-fin array heat sink exposed to an impinging air stream. The pin-fins, which had a square cross-section, were aligned with the air approach

---

* Corresponding author. Tel.: +1 248 370 2489; fax: +1 248 370 4416.
  E-mail address: cjkobus@oakland.edu (C.J. Kobus).

Nomenclature

A	cross-sectional area of fin, $\pi d^2/4$ (m^2)
A_b	base area not occupied by fins, $ab - nA$ (m^2)
a	width of heat sink (m)
b	length of heat sink (m)
c_p	specific heat (J/kg °C)
d	fin diameter (m)
Gr_d	Grashof number
Gr_d^*	modified Grashof number, $r^* Gr_d$
h	convective heat transfer coefficient (W/m^2°C)
k	fin thermal conductivity (W/m °C)
k_f	fluid thermal conductivity (W/m °C)
L	length of fin (m)
m	fin parameter (m^{-1})
n	number of fins
Nu_d	Nusselt number
P'	periphery of fin (m)
P	electrical power (W)
$\dot{Q}_b$	heat transfer from base unoccupied by fins (W)
$\dot{Q}_f$	heat transfer from single fin (W)
$\dot{Q}_s$	heat transfer from entire sink (W)
r'	Reynolds number modifier
r^*	Grashof number modifier
Re_d	Reynolds number
Re_d'	modified Reynolds number, $r' Re_d$
$R_{t,s}$	effective thermal resistance (W/°C)
T_b	base temperature (°C)
T_f	air temperature (°C)
v_f	free stream air velocity (m/s)

Greek symbols

α	void fraction of fin bundle
β	coefficient of thermal expansion (K^{-1})
η_e	fin efficiency
μ	dynamic viscosity (kg/m s)
ρ	air density (kg/m^3)

velocity. The focus of the study was the determination of an optimal fin spacing. Sparrow and Larson [2] experimentally measured heat transfer coefficients for pin-fin arrays when the airflow initially enters the array perpendicular to the fin base. Using naphthalene-coated pin-fins, and the analogy between mass-transfer and convective heat transfer, heat transfer coefficients for individual fins could be indirectly measured. In general, edge-adjacent fins had higher heat transfer coefficients than those situated in the interior of the array. Mina-karni et al. [3] carried out experiments and numerical studies to evaluate the effect of flow-guide vanes on an air-cooling pin-fin array heat sink. The pin-fin array used in the experiments was made of thin square copper pins. Thermal resistance of the heat sink was measured and a design method for the optimum configuration of flow-guide vanes was proposed. Constans et al. [4] carried out a theoretical and numerical study to determine a technique for optimization of a finned heat sink. Heat transfer coefficients were obtained using existing empirical correlations. A finite difference model was developed, and an ellipsoid algorithm used for optimization. You and Chang [5] predicted the convective heat transfer coefficient for pin-fins located in channel flow. The governing differential equations for flow and heat transfer were developed and solved numerically. Sparrow and Vemuri [6] carried out an experimental study on the combined-mode natural convection/radiation heat transfer characteristics of highly populated arrays of pin-fins. The effect of various parameters on thermal performance was investigated. It was found that the

performance increased with fin length. The study revealed the existence of an optimum number of fins for a fixed base plate size. Other research [7–10] has been carried out investigating the thermal performance of pin-fin array heat sinks. Most of the work mentioned above utilized numerical techniques to theoretically determine thermal performance. Also, existing correlations were often used to determine convective heat transfer coefficients.

The purpose of the current research is to formulate as simple a theoretical model as possible capable of predicting the thermal performance characteristics of a pin-fin array heat sink, in terms of various design parameters; which considers the problem in more detail than what was done by Sparrow and Vemuri [7]. Also, to develop an experimental measurement technique that not only can be used to indirectly measure the effective thermal resistance of the heat sink, but the average convective heat transfer coefficient for the fin-bundle as well. Dimensionless heat transfer correlations will be developed from experimental data involving a wide range of design parameters. The value of the simple model, coupled with the heat transfer correlations for the fin-bundle, will be its ability to provide design insight; including the existence of optimum fin spacing.

2. Formulation of theoretical model

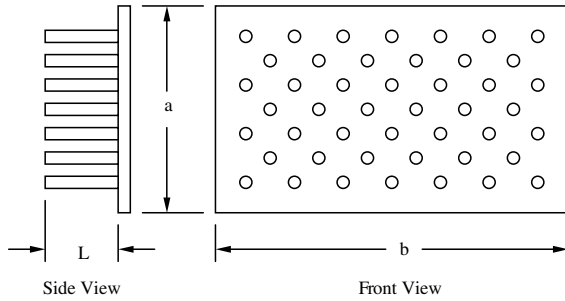A theoretical model for predicting the thermal performance of a pin-fin array heat sink, depicted in

Fig. 1. Schematic of pin fin array heat sink.

Fig. 1, is formulated by considering the heat sink to be made up of a number of individual pin-fins operating in parallel. Therefore, it is necessary to formulate a model governing the rate of heat transfer from an individual pin-fin to air flowing past the fin.

The well-known one-dimensional differential equation governing the temperature distribution for such a fin, covered in most introductory heat transfer textbooks, is given by

$$\frac{d^2 T}{dx^2} - \left(\frac{hP}{kA}\right)(T - T_f) = 0 \tag{1}$$

Solving the resulting differential equation, subject to appropriate boundary conditions, [1] yields the axial temperature distribution in the representative fin. Using this temperature distribution, along with Fourier's model for conduction, the rate of heat transfer from a single pin-fin, $\dot{Q}_f$, can be modeled as

$$\dot{Q}_f = kmA(T_b - T_f)\tanh(mL) \tag{2}$$

where

$$m = \left(\frac{hP'}{kA}\right)^{1/2} \tag{3}$$

and

$$P' = \pi d, \quad A = \frac{\pi d^2}{4} \tag{4}$$

Also, in terms of the convective heat transfer coefficient, the rate of heat transfer from that part of the heat sink base not occupied by fins, $\dot{Q}_b$, can be expressed as

$$\dot{Q}_b = hA_b(T_b - T_f) \tag{5}$$

where

$$A_b = (ab - nA); \quad n = \text{number of fins} \tag{6}$$

Therefore, the total rate of heat transfer from the heat sink, $\dot{Q}_s$, which contains n-fins, can be expressed as

$$\dot{Q}_s = n\dot{Q}_f + \dot{Q}_b \tag{7}$$

Using Eqs. (2), (5), (6) and (7), the effective thermal resistance of the heat sink, $R_{t,s}$, can be modeled as

$$R_{t,s} = \frac{(T_b - T_f)}{\dot{Q}_s}$$

$$= \{n[kmA\tanh(mL)] + h(ab - nA)\}^{-1} \tag{8}$$

The above equation represents a theoretical model for predicting the effective thermal resistance of the heat sink, $R_{t,s}$, in terms of the thermal conductivity of the fin material, k, fin diameter, [2] d, length, L, number of fins, n, area of the heat sink base, ab, and the convective heat transfer coefficient, h, between the fins and the flowing air. For simplicity, it is assumed in the model that the convective heat transfer coefficient, h, is the same for each fin, and also for the base.

With one exception, all of the above physical and thermal parameters are readily obtainable, the exception being the convective heat transfer coefficient, h. The convective heat transfer coefficient is the result of a combination of a number of complex physical mechanisms involving fin geometry, fin spacing, free stream air velocity and direction, buoyancy forces, and fluid properties in addition to the bundle effect. The complexity of the physical mechanisms governing this particular physical parameter is such that they can only partially be modeled. Therefore, in order to determine the required convective heat transfer coefficient, h, for a fin-bundle, there will be the need for developing some form of empirical correlation from appropriate experimental data.

3. Experimental measurement technique

3.1. Reliability of experimental measurement technique

In order to experimentally measure the thermal performance of the finned heat sink, it is essential that the rate of heat transfer between the heat sink and the flowing air be accurately measured. For the present experimental studies of heat sink performance, electrical patch heaters were used to heat the fin base. It would be highly desirable to be able to indirectly obtain an accurate measurement of the rate of heat transfer from the heat sink to the flowing air, by simply measuring the electrical power input to the patch heaters. Equating these two energy rates assumes a negligible heat loss off the back-side and edges of the patch heater assembly.

In order to verify the reliability of this measurement technique, a special experimental set-up was designed to

---

[1] One of the boundary conditions is that the temperature of the fin base is equal to the base temperature. The other boundary condition assumes that the heat flux off the fin tip is negligible.

[2] If the fin is tapered, the average diameter, d, is the arithmetic mean between the tip and the base diameter, $d = (d_t + d_b)/2$.

independently measure both the electrical power input to the patch heaters, P, and the actual rate of heat transfer, $\dot{Q}$, to the air by the heat sink. The latter was done by doing an energy balance on the air as it flowed past the heat sink. The experimental test set-up included the finned heat sink, patch heaters to heat the fin base, a polycarbonate enclosure to provide a uniform air velocity, and to contain the airflow as it flowed past the fins. The backside and edges of the patch heaters were insulated by styrofoam. For all the experimental data obtained, $\dot{Q}$ was less than P as would be expected.

After considerable experimental investigation, it was concluded that the $(P - \dot{Q})$ difference was primarily due to a heat loss through the polycarbonate enclosure and connecting air ducts. This confirmed that the energy had to first be transferred to the flowing air by the finned heat sink. The importance of verifying this is that it provided confidence that the power input, P, to the patch heaters is, for all practical purposes, equal to the rate of heat transfer, $\dot{Q}_s$, from the finned heat sink to the flowing air; thus confirming the reliability of the proposed measurement technique. On the basis of the careful evaluation carried out in this phase of the current research, the measurement of $\dot{Q}_s$ using this technique would always be a little low, with the experimental uncertainty estimated to be less than 5%. This conclusion was similar to that of Sparrow and Vemuri [6] who used a similar apparatus.

3.2. Experimental test set-up

The experimental set-up for indirectly measuring the heat sink performance was different from that described in the previous section. Fig. 2 is a schematic of the experimental test set-up. The set-up included the aluminum fin array heat sink, two 5.1×5.1 cm electric patch heaters to heat the fin base, a plenum chamber and an air-duct to direct the airflow orientation to be such that it flowed perpendicular to the fin base. A copper sheet

was placed in between the patch heaters and the fin base to assure a uniform base temperature. The cross-sectional area of the air-duct was slightly larger than that of the fin base and the duct outlet was positioned about 15.2 cm away from the tip of the fins. The plenum chamber was designed to assure a high degree of uniformity to the air velocity, v_f, leaving the air-duct. For example, for a particular flowrate, fifteen hot-wire anemometer readings over the 111.9 cm^2 duct area yielded an average air velocity of 21.3 cm/s with a standard deviation of ± 1.5 cm/s. The test set-up includes the means for supporting the heat sink/patch heater assembly, the plenum/air-duct assembly, and also includes appropriate instrumentation, which will be discussed in the following section.

3.3. Description of fin geometry, spacing and void fraction

Fin geometry includes tip diameter, d_t, base diameter, d_b, average diameter, d, where $d = (d_t + d_b)/2$, and fin length, L. Fin spacing is shown in Fig. 3, and includes the two dimensions s_1 and s_2. An important parameter associated with correlating the convective heat transfer coefficient for a fin bundle was found to be the fin bundle void fraction, α. The void fraction, α, of a fin-bundle is that fraction of a cross-sectional area of the fin-bundle that is occupied by air. The void fraction can be expressed as

$$\alpha = \left\{ 1 - \frac{2(\pi d^2/4)}{s_1 s_2} \right\} \qquad (9)$$

3.4. Experimental uncertainties

An experimental uncertainty analysis was performed in an effort to discern the accuracy and reliability of the direct and indirect experimental measurements involved. Uncertainties in temperature differences were within ± 0.5 °C, volumetric air flowrates within $\pm 5\%$ of full-

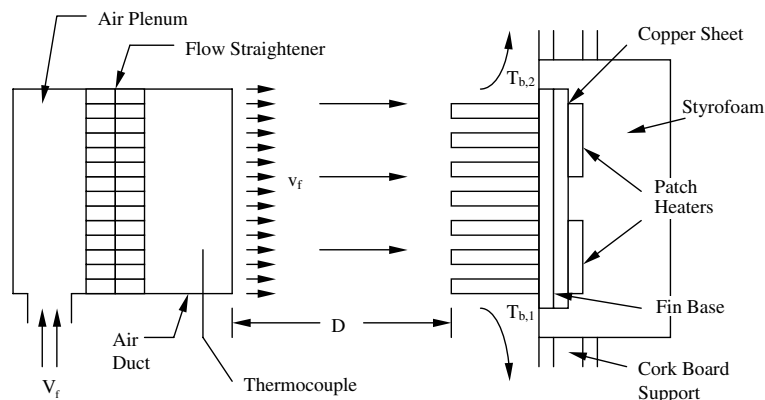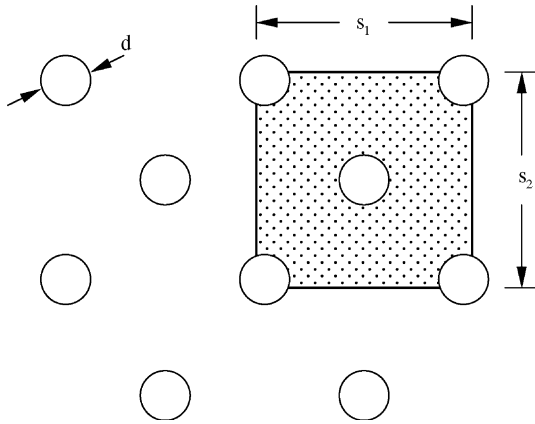

Fig. 2. Schematic of experimental test set-up.

Fig. 3. Fin spacing.

scale readings and power measurements within ±1% of readings. The uncertainty in the indirect effective thermal resistance was determined to be within ±5% of its measured value. A technique for the indirect measurement of the average convective heat transfer coefficient, h, for the fin-bundle was needed, however, since there is no known correlation for fin-bundles, or for different airflow orientations.

3.5. Indirect measurement of convective heat transfer coefficient

Assuming the model represented by Eq. (8) is a reasonable representation of the physical mechanisms involved in the performance of the finned heat sink, and recognizing that the left hand side of the equation can be measured experimentally as a function of air velocity, v_f; then by rearranging Eq. (8), the model provides a means for indirectly measuring the convective heat transfer coefficient, h, as a function of air velocity, v_f. After considerable algebraic manipulation, Eq. (8) can be expressed as

$$h = \frac{\dot{Q}_s}{\{nP'L\eta_e + (ab - nA)\}(T_b - T_f)} \tag{10}$$

where η_e is the fin efficiency defined as

$$\eta_e = \frac{\tanh(mL)}{(mL)}; \quad m = \left(\frac{hP'}{kA}\right)^{1/2} \tag{11}$$

It is recognized that because the fin efficiency, η_e, also involves the convective heat transfer coefficient, h, an iteration scheme must be used to solve for h for each experimental data point, and therefore for each different air velocity, v_f.

An experimental uncertainty analysis was performed to discern the accuracy and reliability of this indirect measurement technique. Knowing the uncertainties in the direct measurements described previously, and then the uncertainties in the indirect measurements, it was determined that the uncertainty in the average convective heat transfer coefficient obtained by using this technique was within ±8% of its measured value.

In addition, it was found that the fin efficiency, η_e, for almost all of the experimental tests was greater than 0.85. Thus, one of the boundary conditions for formulating the theoretical model that assumed a negligible heat flux off the fin tips had to be reconsidered. After considerable investigation, it was determined that, depending upon the number of fins, the rate of heat transfer off the fin tips ranged between 2% and 6% of the total rate of heat transfer from the pin-finned heat sink, $\dot{Q}_s$. The convective heat transfer coefficient, h, was measured indirectly using the theoretical model, and the actual measured total rate of heat transfer from the heat sink, $\dot{Q}_s$. As long as the same model was used to predict the heat sink performance, any model error due to the adiabatic tip assumption would be self-corrective. Therefore, it was concluded that it was better to keep this assumption for the boundary condition since it significantly simplified the theoretical model.

4. Development of a convective heat transfer correlation for air flow perpendicular to the heat sink base (impinging flow)

4.1. Form of dimensionless correlation

The proposed functional form for the convective heat transfer correlation function is the sum of two functions, one which is the result of pure natural convection, $f^*(Gr_d^*)$, and the other which is the result of pure forced convection, $f'(Re_d')$. Therefore, the proposed dimensionless convective heat transfer coefficient correlation function is of the form:

$$\frac{Nu_d}{Pr^{1/3}} = f^*(Gr_d^*) + f'(Re_d') \tag{12}$$

where

$$Gr_d^* = r^* Gr_d = \text{modified Grashof number} \tag{13}$$

and

$$Re_d' = r' Re_d = \text{modified Reynolds number} \tag{14}$$

The dimensionless convective heat transfer coefficient, Nu_d, is the classic Nusselt number, and Pr is the classic Prandtl number. The modifiers r^* and r' each involve fin geometry and fin spacing, and are determined empirically from an experimental database. Gr_d and Re_d are the classical Grashof and Reynolds numbers respectively; thus

$$Nu_d = \frac{hd}{k_f} \tag{15}$$

$$Pr = \frac{\mu c_p}{k_f} \tag{16}$$

$$Gr_d = \frac{\rho^2 g \beta (T_b - T_f) d^3}{\mu^2} \tag{17}$$

$$Re_d = \frac{\rho v_f d}{\mu} \tag{18}$$

4.2. Development of convective heat transfer correlation function for pure natural convection

Utilizing the experimental database for pure natural convection, a correlation function, $f^*(Gr_d^*)$ was empirically developed. After considerable analysis of the experimental data, the form which best fit all of the experimental data was the following power function:

$$f^*(Gr_d^*) = c_0^* (Gr_d^*)^{n^*} \tag{19}$$

where

$$Gr_d^* = r^* Gr_d \tag{20}$$

and the best modifier, r^*, was of the form

$$r^* = (1 - \alpha)^{-1.9} \left(\frac{s_2}{a}\right)^{2.4} \left(\frac{s_1}{b}\right)^{1.4} \left(\frac{d}{L}\right)^{0.8}; \quad s_1 = s_2/2 \tag{21}$$

where

$$c_0^* = 1.141, n^* = 0.230 \tag{22}$$

A graph of the experimentally measured convective heat transfer coefficient as a function of the modified Grashof number is shown in Fig. 4 (Table 1). The empirically determined dimensionless correlation function for pure natural convection, as expressed by Eq. (19), is also depicted. The correlation coefficient for this best fit curve is 0.975. Note that as the modified Grashof number, Gr_d^*, approaches zero, as would be the case when the base-to-air temperature difference, $(T_b - T_f)$, approaches

zero, the dimensionless convective heat transfer coefficient will approach zero, which is physically correct.

4.3. Development of convective heat transfer correlation for pure forced convection

Although it is possible to run experiments for pure natural convection, it is not possible to run experiments for pure forced convection, especially for the velocity ranges under consideration in these studies, $v_f \leqslant 0.61$ m/s. However, in order to achieve the proposed correlation function, as expressed by Eq. (12), it is necessary to somehow "extract" a convective heat transfer coefficient correlation function for pure forced convection from an experimental database of combined forced and natural convection. The technique used, consistent with the proposed form for the combined correlation, is to assume they are relatively independent of each other. Therefore, rearranging Eq. (12), the pure forced convection correlation function, $f'(Re_d')$, can be expressed as

$$f'(Re_d') = \frac{Nu_d}{Pr^{1/3}} - f^*(Gr_d^*) \tag{23}$$

Since the function $f^*(Gr_d^*)$ for pure natural convection is known from Eq. (19), using the experimental database for forced convection, $0 \leqslant v_f \leqslant 0.61$ m/s, it was possible using Eq. (23) to compute values for $f'(Re_d')$ as a function of Re_d'. This resulting data was then used to empirically determine the form of the function $f'(Re_d')$ which best fits all of the data. The result was a third order polynomial of the form:

$$f'(Re_d') = c_0 + c_1 Re_d' + c_2 Re_d'^2 + c_3 Re_d'^3 \tag{24}$$

where the modified Reynolds number is defined as

$$Re_d' = r' Re_d \tag{25}$$

After considerable analysis of the experimental database for pure forced convection, it was determined that the "best" modifier, r', was of the form:

$$r' = \alpha^{2.1} \left(\frac{a}{s_2}\right)^{0.4} \left(\frac{L}{d}\right)^{0.1} \tag{26}$$

The coefficients of the third order polynomial were found to be

$$c_0 = -3.12 \times 10^{-2}, \quad c_1 = -2.99 \times 10^{-3}$$
$$c_2 = 1.46 \times 10^{-4}, \quad c_3 = -3.55 \times 10^{-7} \tag{27}$$

A graph of the experimentally measured [3] dimensionless convective heat transfer coefficient for pure forced convection as a function of the modified Reynolds number is shown in Fig. 5 (Table 2). The empirically determined
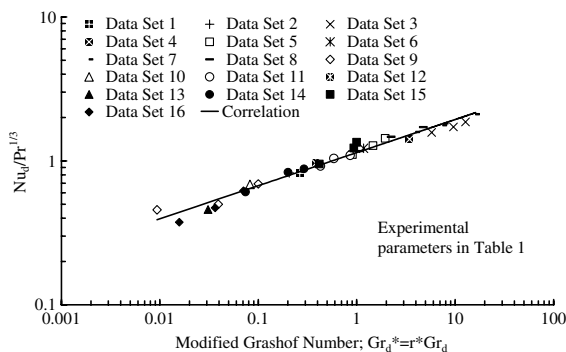

Fig. 4. Empirical correlation of dimensionless convective heat transfer coefficient; pure natural convection.

---

[3] Measured as combined forced and natural convection but corrected to pure forced convection by subtracting off the contribution of pure natural convection.

Table 1
Experimental pin fin array heat sink parameters for Fig. 4

| Data set	d [mm]	L [cm]	s_2 [cm]	n	α	a [cm]	b [cm]
1	3.2	3.2	1.8	132	0.900	14.6	7.6
2	4.4	4.4	1.8	132	0.900	14.6	7.6
3	3.2	3.2	2.3	50	0.939	5.4	12.4
4	3.2	3.2	2.3	87	0.939	7.6	14.6
5	3.2	3.2	1.8	76	0.900	5.4	12.4
6	4.4	4.4	1.8	76	0.900	5.4	12.4
7	4.4	4.4	2.3	50	0.939	5.4	12.4
8	4.4	4.4	2.3	87	0.939	7.6	14.6
9	3.2	3.2	1.3	137	0.804	5.4	12.4
10	4.4	4.4	1.3	137	0.804	5.4	12.4
11	2.0	2.0	1.5	108	0.793	5.4	12.4
12	4.4	4.4	1.8	137	0.900	7.6	14.6
13	4.4	4.4	1.3	230	0.804	7.6	14.6
14	2.0	2.0	1.5	182	0.793	7.6	14.6
15	3.2	3.2	1.8	137	0.900	7.6	14.6
16	3.2	3.2	1.3	230	0.804	7.6	14.6
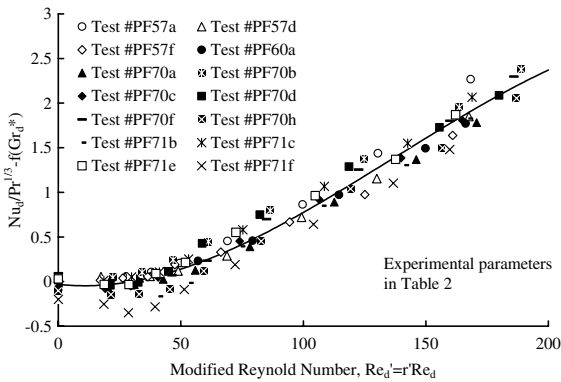
Fig. 5. Empirical correlation of dimensionless convective heat transfer coefficient; pure forced convection.

dimensionless correlation function for pure forced convection, as expressed by Eq. (24), is also depicted. The correlation coefficient for this best fit curve is 0.970.

4.4. Domain of applicability for correlation function

The dimensionless convective heat transfer correlation functions that have been developed above, have been shown to give good results for this particular heat sink geometry and air flow orientation. [4] Also, the accu-

racy of the correlation has only been experimentally verified for the following range of fin, air flow and heat sink parameters: $5.1 \leqslant a \leqslant 14.6$ cm, $5.1 \leqslant b \leqslant 14.6$ cm, $1.3 \leqslant s_2 \leqslant 2.3$ cm, $2.0 \leqslant L \leqslant 4.4$ cm, $2.3 \leqslant d \leqslant 4.1$ mm, $0 \leqslant v_f \leqslant 0.61$ m/s, $s_1 = s_2/2$.

4.5. Determination of convective heat transfer coefficient

The convective heat transfer coefficient, h, for a specific fin geometry and air velocity can be determined by rearranging Eq. (12), thus

$$Nu_d = Pr^{1/3}\left\{f'\left(Re_d'\right) + f^*\left(Gr_d^*\right)\right\} \tag{28}$$

The Nusselt number, as shown in Eq. (15), is expressed in terms of the convective heat transfer coefficient, h, the fin diameter, d, and the thermal conductivity of air, k_f. Therefore, the convective heat transfer coefficient, h, can be determined from Eq. (28) as follows:

$$h = \left(\frac{k_f}{d}\right)Pr^{1/3}\left\{f'\left(Re_d'\right) + f^*\left(Gr_d^*\right)\right\} \tag{29}$$

where $f^*\left(Gr_d^*\right)$ and $f'\left(Re_d'\right)$ are determined from Eqs. (19) and (24) respectively.

5. Predictive capability of theoretical model

5.1. Validation of theoretical model with experimental data

The validity of the theoretical model, represented by Eq. (8), is best tested by comparing its predictive

---

[4] It is important to recognize that all of the experimental data used in developing the correlation function are for the specific gravitational and airflow orientation shown in Fig. 2, with $D = 15.2$ cm.

Table 2
Experimental pin fin array heat sink parameters for Fig. 5

Data set	d [mm]	L [cm]	s_2 [cm]	n	α	a [cm]	b [cm]
PF57a	3.9	2.0	1.5	108	0.793	5.4	12.4
PF57d	3.2	4.4	1.3	137	0.804	5.4	12.4
PF57f	3.2	3.2	1.3	137	0.804	5.4	12.4
PF60a	3.9	2.0	1.5	182	0.793	7.6	14.6
PF70a	3.2	4.4	1.3	230	0.804	7.6	14.6
PF70b	3.2	4.4	1.8	137	0.900	7.6	14.6
PF70c	3.2	3.2	1.3	230	0.804	7.6	14.6
PF70d	3.2	3.2	1.8	137	0.900	7.6	14.6
PF70f	3.2	4.4	2.3	87	0.939	7.6	14.6
PF70h	3.2	3.2	2.3	87	0.939	7.6	14.6
PF71b	3.2	4.4	2.3	50	0.939	5.4	12.4
PF71c	3.2	4.4	1.8	76	0.900	5.4	12.4
PF71e	3.2	3.2	1.8	76	0.900	5.4	12.4
PF71f	3.2	3.2	2.3	50	0.939	5.4	12.4

capability to actual experimental measurements. Therefore, the measured thermal performance for many different finned heat sinks having a wide range of fin and base parameters are compared with their theoretically predicted thermal performance by plotting the effective thermal resistance, $R_{t,s}$, as a function of air velocity, v_f, flowing perpendicular to the heat sink base (impinging flow). From this wide range of data, the measured thermal performance for four different fin geometries and fin spacings are chosen and plotted in Fig. 6 (Table 3). Also, superimposed in Fig. 6 is the effective thermal resistance, $R_{t,s}$, of the four different heat sinks as predicted by the theoretical model. As can be seen, the predictive capability of the theoretical model is exceptionally good over the range of parameters; especially when consideration is given to the simplicity of the model, and the complexity of the physical mechanisms involved.
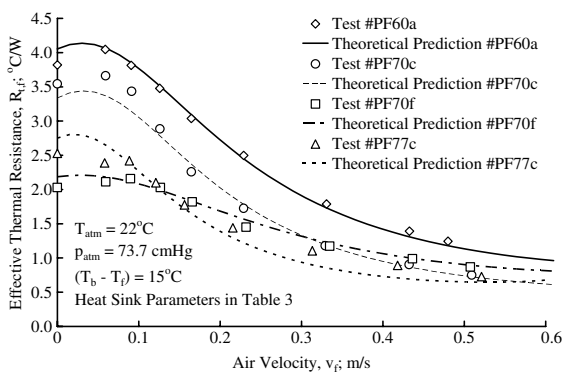

Fig. 6. Thermal performance of pin fin array heat sinks; comparison with theoretical prediction.

6. Design insight obtained from theoretical model

The theoretical model, in conjunction with the developed convective heat transfer correlation was used to carry out a parametric study of the influence of various design parameters on the thermal performance of the heat sink.

6.1. Influence of fin diameter

It was found that a change in diameter has relatively little influence on the effective thermal resistance of the heat sink for air velocities, v_f, greater than 0.25 m/s. For velocities less than 0.25 m/s, where natural convection starts to dominate the heat transfer mechanism, a smaller diameter yields a slightly better overall thermal performance of the heat sink. This difference in thermal performance is less than 6%, where fin diameters differed from each other by more than 25%. Therefore, it was concluded that for a given fin spacing, fin performance, $R_{t,s}$, is only a weak function of fin diameter, d. This suggests that the convective heat transfer coefficient must increase as the diameter decreases in such a way as to offset the detrimental effect of the decrease in heat transfer surface area.

6.2. Influence of fin length

The theoretical model was again used to carry out a parametric study of the influence of fin length on the thermal performance of the heat sink. The results of the study are depicted in Fig. 7 (Table 4). The fixed heat sink parameters are specified, and four sets of data are shown. Test #PF70a and PF70c have the same finned heat sink parameters, which include a fin spacing,

Table 3
Experimental pin fin array heat sink parameters for Fig. 6

Data set	d [mm]	L [cm]	s_2 [cm]	n	α	a [cm]	b [cm]
PF60a	3.9	2.0	1.5	182	0.793	7.6	14.6
PF70c	3.2	3.2	1.3	230	0.804	7.6	14.6
PF70f	3.2	4.4	2.3	87	0.939	7.6	14.6
PF77c	3.2	4.4	1.8	132	0.900	14.6	7.6

$s_2 = 1.3$ cm. Only the length, L, is different. Also, Test #PF70b and PF70d have the same finned heat sink parameters, which include a fin spacing, $s_2 = 1.8$ cm. Again, only the fin lengths are different. In addition, note that the fin length used for both Test #PF70a and #PF70b was 4.4 cm, and the fin length used for both Test #PF70c and #PF70d was 3.2 cm. The result shows that as the fin length increases, the effective thermal resistance decreases, which corresponds to an increase in performance. At air velocities less than 0.15 m/s, where natural convection starts to dominate the heat transfer mechanism, the effective thermal resistance decreased more than 16% when the fin length was increased by 40%. This was true for both fin spacings. Therefore, it was concluded that the thermal performance of the finned heat sink is improved when fin length is increased.

It should be pointed out, however, that there seems to be a point of diminishing return with respect to increasing fin length. The physical mechanism for this characteristic must be that the fin efficiency, η_e, decreases as the fin length increases, which in part offsets, thermal performance wise, the fact that the convective heat transfer surface area increases as the fin length increases. For the domain of diameter and fin spacing used in this study, the point of diminishing return seems to start when the fin length exceeds 4.7 cm.
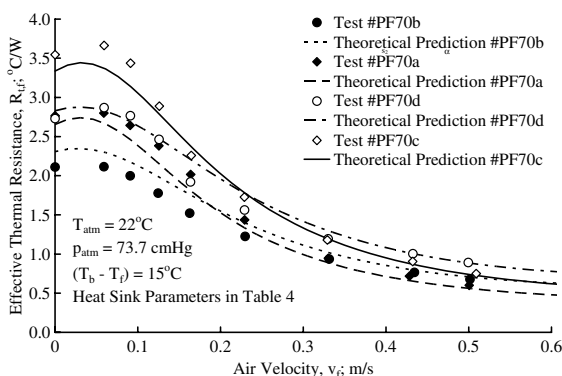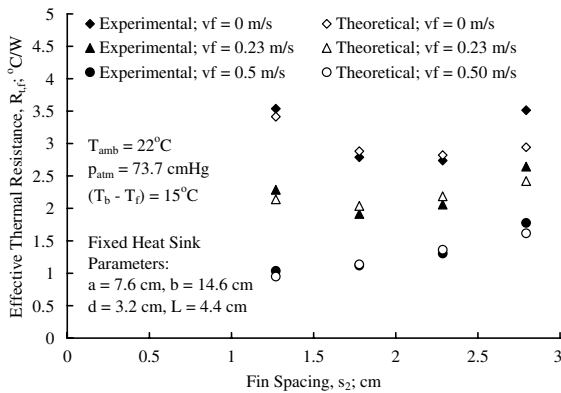

Fig. 7. Thermal performance of pin fin array heat sinks; influence of fin length; comparison with theoretical prediction.

6.3. Influence of fin spacing

The theoretical model was again used to carry out the parametric study to investigate the influence of fin spacing, s_2, on the thermal performance of the finned heat sink. Heat sinks with four different spacings, but with the same fin diameter and length, were tested and compared. The four different fin spacings [5] used for the heat sink bases were $s_2 = 1.3$ cm, 1.8 cm, 2.3 cm and 2.8 cm. Fig. 8 depicts the very interesting result. The theoretical predictions and the experimental data confirms the existence of an optimum fin spacing. For pure natural convection, $v_f = 0$ m/s, and for this particular base size and fin parameters, the optimum spacing appears to be, $s_2 = 2.3$ cm. Although it is not as pronounced, at a velocity, $v_f = 0.23$ m/s, the optimum fin spacing appears to be $s_2 = 1.8$ cm. As can be seen from Fig. 8, however, such an optimum spacing does not exist for a velocity, $v_f = 0.50$ m/s. The above series of experiments were repeated with the different fin lengths and base sizes. The fin lengths tested were $L = 4.4$ and 3.2 cm, and the base sizes tested were $a = 7.6$ cm, $b = 14.6$ cm and $a = 5.4$ cm, $b = 12.4$ cm. Again the optimal fin spacing appears to be $1.8 \leqslant s_2 \leqslant 2.3$ cm, although it was not as pronounced for the smaller sized base. These results have considerable practical significance as it relates to the design of an efficient finned heat sink.

The physics behind the above observed thermal performance behavior is as follows: increasing the fin spacing, s_2, for a fixed heat sink base area decreases the number of fins and thus the heat transfer surface area. However, especially in the near natural convection domain, $v_f < 0.24$ m/s, increasing the fin spacing also decreases the fin bundle effect, which in turn increases the convective heat transfer coefficient. For the large size heat sinks tested above, as the fin spacing, s_2, increases from 1.3 cm to 1.8 cm, the convective heat transfer coefficient apparently increases faster than the fin surface area decreases, thus causing the thermal performance to increase. When the fin spacing increases much beyond $s_2 = 1.8$ cm, however, the convective heat transfer coefficient apparently no longer increases as fast as the fin's

---

[5] The fin pattern is shown in Fig. 3. For all of the fins tested, $s_1 = s_2/2$.

Table 4
Experimental pin fin array heat sink parameters for Fig. 7

Data set	d [mm]	L [cm]	s_2 [cm]	n	α	a [cm]	b [cm]
PF70a	3.2	4.4	1.3	230	0.804	7.6	14.6
PF70b	3.2	4.4	1.8	137	0.900	7.6	14.6
PF70c	3.2	3.2	1.3	230	0.804	7.6	14.6
PF70d	3.2	3.2	1.8	137	0.900	7.6	14.6

Fig. 8. Thermal performance of pin fin array heat sinks; influence of fin spacing; comparison with theoretical prediction.

surface area decreases, thus causing the thermal performance to begin dropping off.

As can be seen in Fig. 8, good agreement is seen to exist between the theoretical prediction and experimental data, especially when consideration is given to the simplicity of the model, and the complexity of the physical mechanisms involved. It is noted, however, that the theoretical predictions for fin spacing, $s_2 > 2.5$ cm, are not as accurate. One of the reasons for this inaccuracy is that it has not been possible to get a good dimensionless empirical correlation for the convective heat transfer coefficient for these higher fin spacings. This is because, for $s_2 > 2.5$ cm, the ratio of fin surface area to heat sink base area becomes less than 1.6, whereas for $s_2 = 1.3$ cm, the area ratio is 6.6. Thus, the dominant heat transfer shifts from that associated with the fins to that associated with the base for fin spacings $s_2 > 2.5$ cm. This limitation should not be a problem, however, since all practical fin geometries would involve fin spacings $s_2 \leqslant 2.5$ cm.

7. Summary and conclusions

A comprehensive theoretical and experimental study was carried out on the thermal performance of a pin-fin array heat sink. The study resulted in the successful development of a theoretical model that has the capability of predicting the influence of various physical, thermal, and flow parameters on the effective thermal resistance of a pin-fin array heat sink. The value of the theoretical model is that it can be used as a significant design tool to determine the influences of various design parameters such as fin diameter, length and spacing; base size, configuration and temperature; and air flow orientation, velocity and temperature on the effective thermal resistance of the heat sink. The form of the theoretical model came out to be quite simple despite of the complexity of the physical mechanism involved in this study. It was expressed in terms of various physical and thermal parameters, all of which were readily obtainable with one exception. The exception was the convective heat transfer coefficient. In order to determine the convective heat transfer coefficient for a fin array heat sink, it required some form of empirical correlation from appropriate experimental data.

The experimental measurement technique for the thermal performance of a finned heat sink was developed, and many experiments with a wide range of parameters were carried out for pure natural convection and for combined natural and forced convection. Effective thermal resistance of a fin array heat sink was indirectly measured as a function of free stream air velocity, which was perpendicular to the heat sink base (impinging). Also, the convective heat transfer coefficient of a fin array heat sink was indirectly measured using the theoretical model derived, as a function of free stream air velocity.

A dimensionless convective heat transfer correlation for a fin array heat sink was developed from the experimental data obtained. The form of the dimensionless correlation consisted of the sum of two convective heat transfer correlation functions; one for pure natural convection and the other for pure forced convection. The dimensionless convective heat transfer correlation was used in conjunction with the theoretical model to predict the thermal performance of a fin array heat sink.

The predictive capability of the theoretical model was verified by comparing with experimental data for many different fin array heat sinks having a wide range of fin and base parameters. The predictive capability of the theoretical model was shown to be exceptionally good over the range of parameters, especially when consideration is give to the simplicity of the model, and the complexity of the physical mechanisms involved.

Utilizing the theoretical model and experimental data, the influence of different fin parameters, such as fin diameter, length, and spacing, on the effective thermal resistance was investigated. The study concluded that for a given fin spacing, thermal performance of a fin array heat sink is only a weak function of fin diameter, and it is improved when fin length is increased. It is also pointed out that there seems to be a point of diminishing return with respect to increasing fin length. The study also uncovered the existence of an optimum fin spacing, $s_2 = 1.8$ cm, for this particular airflow configuration.

Acknowledgments

References

[1] G. Ledezma, A.M. Morega, A. Bejan, Optimal spacing between pin fins with impinging flow, ASME J. Heat Transfer 118 (1996) 570–577.

[2] E.M. Sparrow, E.D. Larson, Heat transfer from pin-fins situated in an oncoming longitudinal flow which turns to crossflow, Int. J. Heat Mass Transfer 25 (5) (1982) 603–614.

[3] K. Minakarni, K. Hisano, H. Iwasaki, S. Mochizuki, Application of the pin-fin heat sink to electronic equipment [Study on design method for flow-guide vanes], Appl. CAFJCAD Electron. Syst. ASME EEP-18 (1996) 117–122.

[4] E.W. Constans, A.D. Belegundu, A.K. Kulkarni, Optimization of a pin-fin sink: a design tool, CAFJCAD Appl. Electron. Packaging ASME EEP-9 (1994) 25–32.

[5] H.I. You, C.-H. Chang, Numerical prediction of heat transfer coefficient for a pin-fin channel flow, ASME J. Heat Transfer 119 (1997) 840–843.

[6] E.M. Sparrow, S.B. Vemuri, Natural convection–radiation heat transfer from highly populated pin-fin arrays, ASME J. Heat Transfer 107 (1985) 190–197.

[7] C.L. Chapman, S. Lee, B.L. Schmidt, Thermal performance of an ellipticcu pin fin heat sink, in: Tenth Annual IEEE Semiconductor Thermal Measurement and Management Symposium, 1994, pp. 24–31.

[8] K. Minakarni, M. Ishizuka, S. Mochizuki, Performance evaluation of pin-fin heat sinks utilizing a local heating method, J. Enhanced Heat Transfer 2 (1–2) (1995) 17–22.

[9] Y. Kondo, H. Matsushima, Prediction algorithm of thermal resistance in the case of pin-fin heat sinks for LSI packages using impingement cooling, Nihon Kikaigakkai Ronbunshu (B-hen) 62 (595) (1996) 332–339.

[10] W.W. Lin, D.J. Lee, Second-law analysis on a pin-fin array under crossflow, Int. J. Heat Mass Transfer. 40 (8) (1997) 1937–1945.